Dalton
www.rsc.org/dalton

Synthesis and reactivity of icosahedral molybdenum-monocarbaborane complexes containing one or two intramolecular amino bridges †

Shaowu Du, Jason A. Kautz, Thomas D. McGrath and F. Gordon A. Stone
Department of Chemistry & Biochemistry, Baylor University, Waco, Texas 76798-7348, USA

Received 3rd September 2002, Accepted 18th November 2002
First published as an Advance Article on the web 9th December 2002

The room-temperature reaction of $Li_2[7\text{-}NMe_3\text{-}nido\text{-}7\text{-}CB_{10}H_{10}]$ with $[Mo(CO)_4\{NH(CH_2)_5\}_2]$ in THF (THF = tetrahydrofuran), followed by oxidation with CF_3SO_3Me or $CH_2{=}CHCH_2Br$, gives the anion $[2,3\text{-}\mu\text{-}\{N(CH_2)_5\}\text{-}2,2,2\text{-}(CO)_3\text{-}closo\text{-}2,1\text{-}MoCB_{10}H_{10}]^-$, isolated as the $[N(PPh_3)_2]^+$ salt **3a**. This salt may similarly be isolated following the direct reaction of $7\text{-}NMe_3\text{-}nido\text{-}7\text{-}CB_{10}H_{12}$ with $[Mo(CO)_4\{NH(CH_2)_5\}_2]$ in refluxing THF. An X-ray diffraction study confirmed the absence of the *C*–NMe_3 group in the anion and formation of an intramolecular piperidinyl bridge between molybdenum and boron. The related compound $[N(PPh_3)_2][1\text{-}NH_2\text{-}2,3\text{-}\mu\text{-}\{N(CH_2)_5\}\text{-}2,2,2\text{-}(CO)_3\text{-}closo\text{-}2,1\text{-}MoCB_{10}H_9]$ **4** is obtained from $Li[7\text{-}NH_2\text{-}nido\text{-}7\text{-}CB_{10}H_{12}]$ with $[Mo(CO)_4\{NH(CH_2)_5\}_2]$ in refluxing THF. Treatment of **3a** or **4** with $\{M(PPh_3)\}^+$ (M = Cu, Ag) yields heterobimetallic complexes containing direct Mo–M bonds, of which $[2,7,11\text{-}\{Cu(PPh_3)\}\text{-}7,11\text{-}(\mu\text{-}H)_2\text{-}2,3\text{-}\mu\text{-}\{N(CH_2)_5\}\text{-}2,2,2\text{-}(CO)_3\text{-}closo\text{-}2,1\text{-}MoCB_{10}H_8]$ has been studied by X-ray diffraction analysis. In THF solution, **4** is oxidized by iodine or *N*-chlorosuccinimide affording the Mo^{IV} species $[1,2\text{-}\mu\text{-}NH_2\text{-}2,3\text{-}\mu\text{-}\{N(CH_2)_5\}\text{-}2,2,2\text{-}(CO)_2\text{-}2\text{-}X\text{-}closo\text{-}2,1\text{-}MoCB_{10}H_9]$ (X = I, Cl, respectively). An X-ray diffraction study of the iodo derivative showed that it contained *two* intramolecular amino bridges between cage vertices and molybdenum. Treatment of these species with PEt_3 in refluxing THF leads to displacement of a carbonyl ligand rather than an amino bridge.

As part of our investigation of the reactions of transition-metal carbonyl complexes of the monocarbollide $[nido\text{-}7\text{-}CB_{10}H_{11}]^{3-}$ ligand,[1,2] we became interested in extending this chemistry to include derivatives of the charge-compensated carbaboranes $7\text{-}NR_3\text{-}nido\text{-}7\text{-}CB_{10}H_{12}$ (R = H, alkyl).[3] Our initial studies showed that the amines attached to the cage-carbon atom could also participate in the coordination of metal-carbonyl fragments. For example, the *C*-amine substituted carbaborane $7\text{-}NH_2Bu^t\text{-}nido\text{-}7\text{-}CB_{10}H_{12}$ is readily deprotonated to form the monoanion $[7\text{-}NHBu^t\text{-}nido\text{-}7\text{-}CB_{10}H_{12}]^-$, which reacts with $[Mo(CO)_6]$ in refluxing NCMe to give $[1,2\text{-}\mu\text{-}NHBu^t\text{-}2,2,2\text{-}(CO)_3\text{-}closo\text{-}2,1\text{-}MoCB_{10}H_{10}]^-$, isolated as the $[N(PPh_3)_2]^+$ salt **1a**.[4] In this complex the exopolyhedral $NHBu^t$ group forms a bridge between the cage-carbon atom and molybdenum. However, with $[7\text{-}NH_2\text{-}nido\text{-}7\text{-}CB_{10}H_{12}]^-$ under the same conditions, **1b** was not obtained. Instead, coupling of NCMe with the cage-bound NH_2 group occurs affording the species $[1,2\text{-}\mu\text{-}\{NHC(Me){=}NH\}\text{-}2,2,2\text{-}(CO)_3\text{-}closo\text{-}2,1\text{-}MoCB_{10}H_{10}]^-$, in which the amidine group bridges between the cage-carbon and molybdenum atoms.[5] On the other hand, the dianion $[7\text{-}NMe_3\text{-}nido\text{-}7\text{-}CB_{10}H_{10}]^{2-}$ reacts with $[Mo(CO)_3(NCMe)_3]$, followed by oxidation with $CH_2{=}CHCH_2Br$ or I_2, to give the anions $[2,2,2\text{-}(CO)_3\text{-}2\text{-}X\text{-}3\text{-}NMe_3\text{-}closo\text{-}2,1\text{-}MoCB_{10}H_{10}]^-$, isolated as $[N(PPh_3)_2]^+$ salts **2a** (X = Br) and **2b** (X = I), respectively.[6] During the course of the latter reactions the NMe_3 group migrates from carbon to an adjacent boron atom in the $\overline{CBBBB}$ belt of the carbaborane ligand. In contrast, in a parallel reaction employing $[Mo(CO)_3(NCMe)_2(PPh_3)]$, the NMe_3 group is simply lost, giving the monoanion $[2,2,2\text{-}(CO)_3\text{-}2\text{-}PPh_3\text{-}closo\text{-}2,1\text{-}MoCB_{10}H_{11}]^-$.[6]

These differences in reactivity of the anions derived by deprotonating various carbaboranes $7\text{-}NR_3\text{-}nido\text{-}7\text{-}CB_{10}H_{12}$ towards different molybdenum carbonyl complexes prompted us to study their reactions with other common molybdenum reagents. In the present study, $[Mo(CO)_4\{NH(CH_2)_5\}_2]$ was used as the precursor to several new molybdenacarbaboranes containing one or two intramolecular amino groups that bridge between cage vertices and the molybdenum centre.

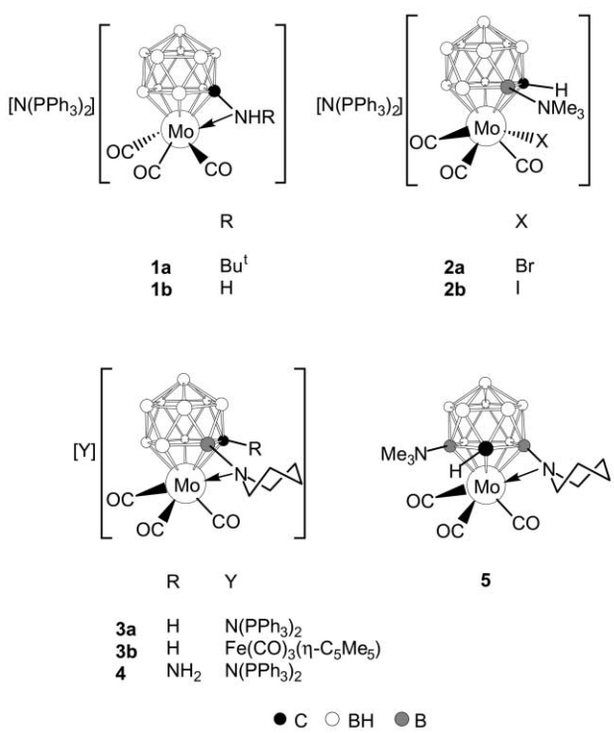

Chart 1

Results and discussion

As mentioned above, in an earlier study we found that reaction of the dianion $[7\text{-}NMe_3\text{-}nido\text{-}7\text{-}CB_{10}H_{10}]^{2-}$ with $[Mo(CO)_3$-

† The new compounds described herein are based upon *closo*-1-carba-2-molybdenadodecaborane fragments, and all bear boron-bound exopolyhedral substituents. It should be noted that, although they contain chiral centres, species here occur as racemates. Substitued boron atoms at positions 3, 7, 11 or 6 could equally be labeled 6, 11, 7 and 3, respectively. In each case the former is used, in accordance with IUPAC convention.

DOI: 10.1039/b208584b

$(NCMe)_3$], followed by oxidation with CH_2=$CHCH_2Br$ or I_2, yielded compounds **2**, where the NMe_3 group migrated from the carbon atom in the cage to an adjacent boron atom on the C*B*BB*B* face that ligates molybdenum.[6] In parallel investigations, $[Mo(CO)_4\{NH(CH_2)_5\}_2]$ was treated with the dianion $[7\text{-}NMe_3\text{-}nido\text{-}7\text{-}CB_{10}H_{10}]^{2-}$ and the presumed Mo^0 intermediate then oxidized with CH_2=$CHCH_2Br$ or CF_3SO_3Me. However, these reactions unexpectedly did not give compounds of type **2** nor any species of formulation $[2,2,2\text{-}(CO)_3\text{-}2\text{-}\{NH(CH_2)_5\}\text{-}n\text{-}NMe_3\text{-}closo\text{-}2,1\text{-}MoCB_{10}H_{10}]$ (n = 1 or 3). Instead, the product obtained following addition of $[N(PPh_3)_2]Cl$ and chromatography was $[N(PPh_3)_2][2,3\text{-}\mu\text{-}\{N(CH_2)_5\}\text{-}2,2,2\text{-}(CO)_3\text{-}closo\text{-}2,1\text{-}MoCB_{10}H_{10}]$ **3a**. The same salt was subsequently also isolated – albeit in lower yield – from the reaction between $[Mo(CO)_4\{NH(CH_2)_5\}_2]$ and $7\text{-}NMe_3\text{-}nido\text{-}7\text{-}CB_{10}H_{12}$ or salts of $[nido\text{-}7\text{-}CB_{10}H_{13}]^-$ in refluxing THF. Conversely, when the same molybdenum reagent was similarly treated with the carbaborane anions $[7\text{-}NHR\text{-}nido\text{-}7\text{-}CB_{10}H_{12}]^-$ (R = Bu^t, H) in refluxing THF, it had been thought that compounds **1** could be formed. For R = Bu^t, this was indeed the case. However, for R = H, **1b** was again not observed. Instead, the only product isolated from this reaction after addition of $[N(PPh_3)_2]Cl$ was $[N(PPh_3)_2][1\text{-}NH_2\text{-}2,3\text{-}\mu\text{-}\{N(CH_2)_5\}\text{-}2,2,2\text{-}(CO)_3\text{-}closo\text{-}2,1\text{-}MoCB_{10}H_9]$ **4**.

Although the presence of the bridging piperidinyl group in the anions of **3a** and **4** could readily be inferred from the NMR data (discussed below), it could not be confirmed without X-ray diffraction studies. Attempts to grow crystals of **3a** or **4** suitable for X-ray analysis were unsuccessful. However, a structure determination of the compound **3b**, an unexpected product obtained from the reaction of **3a** with the cation $[Fe(CO)_2(THF)(\eta\text{-}C_5Me_5)]^+$, has been carried out. The structure of one of the crystallographically-independent anions of **3b**, together with selected bond lengths and angles, is shown in Fig. 1. The

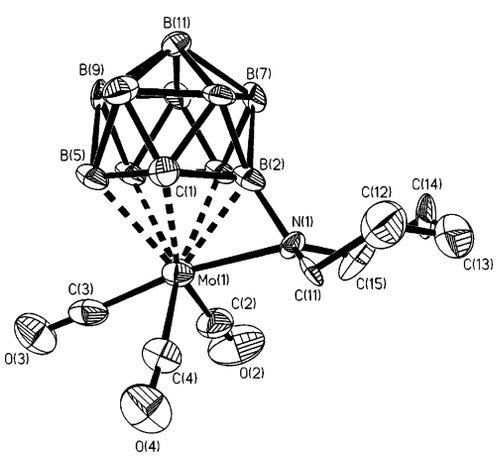

Fig. 1 Structure of one of the crystallographically-independent anions of **3b** showing the crystallographic labeling scheme; the other is geometrically very similar. Hydrogen atoms are omitted and thermal ellipsoids are drawn at the 40% probability level. Selected bond lengths (Å) and angles (°): Mo(1)–C(1) 2.370(15), Mo(1)–C(2) 1.93(2), Mo(1)–C(3) 1.98(2), Mo(1)–C(4) 1.97(2), Mo(1)–N(1) 2.291(13), Mo(1)–B(2) 2.24(2), Mo(1)–B(3) 2.39(2), Mo(1)–B(4) 2.45(2), Mo(1)–B(5) 2.39(2), B(2)–N(1) 1.46(2); C(2)–Mo(1)–N(1) 94.9(7), C(3)–Mo(1)–N(1) 169.6(6), C(4)–Mo(1)–N(1) 91.4(6), N(1)–Mo(1)–C(1) 70.8(5), B(2)–N(1)–Mo(1) 69.3(9).

open face of the $8\text{-}\{N(CH_2)_5\}\text{-}nido\text{-}7\text{-}CB_{10}H_{10}$ fragment is coordinated to the molybdenum atom in a conventional *pentahapto* manner. Its exopolyhedral $N(CH_2)_5$ moiety is also bonded to the metal [Mo–N(1) = 2.291(13), B(2)–N(1) = 1.46(2) Å, B(2)–N(1)–Mo = 69.3(9)°]. The Mo–B(2) bond length [2.24(2) Å] is much shorter than those between Mo and the other atoms in the CBBBB ring [2.39(2) to 2.45(2) Å], indicating some slippage of the metal atom toward B(2) to accommodate the intramolecular Mo–N(1) bond. Similar slippage of the metal towards the cage-carbon atom was found in the tungsten analogue of **1a**.[4] To satisfy the 18-electron configuration of the Mo^{II} (d^4) centre, the $[8\text{-}\{N(CH_2)_5\}\text{-}nido\text{-}7\text{-}CB_{10}H_{10}]^{3-}$ fragment donates eight electrons ($6\pi + 2\sigma$) to the valence shell and the three CO ligands contribute the other six. Although compounds **1** contain an intramolecular NHR bridge between molybdenum and the cage-carbon atom, such a bonding mode for an exopolyhedral amino substituent between a cage-boron and the metal centre, as seen in **3** and **4**, has not been reported previously. However, similar structures where an iodide connects the molybdenum and a cage-boron vertex have been seen, for instance, in the compounds $[2,2,2\text{-}(CO)_3\text{-}2,3\text{-}\mu\text{-}I\text{-}n\text{-}L\text{-}closo\text{-}2,1\text{-}MoCB_{10}H_9]$ (n = 7, 11; L = thioethers).[7] Perhaps significantly, in the latter species, as in **3** and **4**, it is an α-boron atom in the C*B*BB*B* belt that is involved in the intramolecular bridge.

Microanalytical and spectroscopic data characterizing compounds **3a** and **4** are listed in Tables 1–3. The IR spectra of **3a** and **4** both display three CO stretching bands at nearly the same frequencies, in agreement with their similar structures. The $^{11}B\{^1H\}$ NMR spectra of **3a** and **4** both show nine peaks, of which only one in each case is of intensity 2 due to a coincidence, indicating the high asymmetry of the cage. In the fully coupled ^{11}B spectra, the signals at δ 9.9 (**3a**) and 12.6 (**4**) remain as singlets and are attributed to the boron nuclei carrying the piperidinyl group. The chemical shift of this boron atom is typical for *B*-amine features in related compounds.[2f,6] In the ^1H NMR spectra of **3a** and **4**, the signals due to the piperidinyl fragment are found as several multiplets in the ranges δ 3.19 to 1.27 for **3a** and δ 4.35 to 1.52 for **4**. A very broad signal at δ 2.12 in the ^1H NMR of **3a** can be assigned as the cage CH resonance. The resonance of the NH_2 group that is attached to the cage-carbon atom in **4** is recognized as a broad singlet at δ 2.00. In each of the $^{13}C\{^1H\}$ NMR spectra a broad resonance is seen for the cage C atom, at δ 53.2 (**3a**) and 87.7 (**4**).

A possible reaction pathway for the formation of the anion of compounds **3** is indicated in Scheme 1. As reported previously,[6] oxidation of the Mo^0 dianion **A** with CH_2=$CHCH_2Br$ or CF_3SO_3Me would afford the neutral Mo^{II} complex **B** with a vacant coordination site at the Mo centre, which then acquires a piperidine ligand from solution to form the electronically saturated compound **C**. Next, the C–NMe_3 unit in **C** is converted to C–H by NMe_3 loss *via* **D** and gain of H^- from the medium giving the anion **E**. The acidic N–H of the piperidine then abstracts H^- from an $\alpha\ ^{\delta+}B\text{–}H^{\delta-}$ vertex of the cage to eliminate H_2 and form the intramolecular B–N–Mo piperidinyl bridge in **F**, the anion of compounds **3**. When $7\text{-}NMe_3\text{-}nido\text{-}7\text{-}CB_{10}H_{12}$ reacts with $[Mo(CO)_4\{NH(CH_2)_5\}_2]$ in refluxing THF, intermediate **C** is formed *via* H_2 elimination and then follows the same route to afford **F**. Although unusual, the conversion of **C** to **E** described above is not unprecedented: we have noted previously that neutral complexes formed between the $[7\text{-}NMe_3\text{-}nido\text{-}7\text{-}CB_{10}H_{10}]^{2-}$ ligand and $\{Mo(CO)_3L\}^{2+}$ fragments appear to be unstable with respect to a similar C–NMe_3 to C–H conversion.[6]

In parallel with compounds **3**, the formation of the anion of **4** (Scheme 2) likely proceeds *via* initial formation of an intermediate **G** (R = H). Elimination of H_2 from **G** again produces a piperidinyl group bridging between a cage α-boron atom and the molybdenum centre, as seen in **H**, which is the anion of **4**. It is reasonably assumed that **J**, the anion of **1a**, is formed through a related intermediate **G**, with R = Bu^t, from which the molybdenum-bound piperidine is simply displaced by an intramolecular donor bond from the $NHBu^t$ group bound to the cage-carbon.

Two further reactions were carried out which are relevant to some aspects of the reaction pathways described above. Compound **3a** could also be isolated in good yield from treatment of $[N(PPh_3)_2][2,2,2,2\text{-}(CO)_4\text{-}closo\text{-}2,1\text{-}MoCB_{10}H_{11}]$[2d] with Me_3NO

Table 1 Analytical and physical data

Compound		Colour	Yield (%)	ν_{max}(CO) [a]/cm^{-1}	Analysis (%) [b] C	H	N
3a	$[N(PPh_3)_2][2,3\text{-}\mu\text{-}\{N(CH_2)_5\}\text{-}2,2,2\text{-}(CO)_3\text{-}closo\text{-}2,1\text{-}MoCB_{10}H_{10}]$	pink	44	1994 vs, 1924 m, 1873 s	58.1 (57.9)	5.6 (5.4)	2.9 (3.0)
4	$[N(PPh_3)_2][1\text{-}NH_2\text{-}2,3\text{-}\mu\text{-}\{N(CH_2)_5\}\text{-}2,2,2\text{-}(CO)_3\text{-}closo\text{-}2,1\text{-}MoCB_{10}H_9]$	violet	25	1992 vs, 1922 m, 1874 s	57.2 (57.0)	5.5 (5.4)	4.5 (4.4)
5	$[2,3\text{-}\mu\text{-}\{N(CH_2)_5\}\text{-}2,2,2\text{-}(CO)_3\text{-}6\text{-}NMe_3\text{-}closo\text{-}2,1\text{-}MoCB_{10}H_9]$	violet	55	2008 vs, 1930 m, 1910 s	31.8 (31.9)	6.2 (6.2)	6.2 (6.2)
6	$[2,7,11\text{-}\{Cu(PPh_3)\}\text{-}7,11\text{-}(\mu\text{-}H)_2\text{-}2,3\text{-}\mu\text{-}\{N(CH_2)_5\}\text{-}2,2,2\text{-}(CO)_3\text{-}closo\text{-}2,1\text{-}MoCB_{10}H_8]$	violet	58	2014 vs, 1963 m, 1893 s	41.8 (41.8) [c]	4.7 (4.6)	1.7 (1.7)
7	$[2,7,11\text{-}\{Cu(PPh_3)\}\text{-}7,11\text{-}(\mu\text{-}H)_2\text{-}1\text{-}NH_2\text{-}2,3\text{-}\mu\text{-}\{N(CH_2)_5\}\text{-}2,2,2\text{-}(CO)_3\text{-}closo\text{-}2,1\text{-}MoCB_{10}H_7]$	violet	55	2015 vs, 1963 m, 1896 s	43.4 (43.3) [d]	5.0 (4.9)	3.7 (3.7)
8	$[2,11\text{-}\{Ag(PPh_3)\}\text{-}11\text{-}\mu\text{-}H\text{-}2,3\text{-}\mu\text{-}\{N(CH_2)_5\}\text{-}2,2,2\text{-}(CO)_3\text{-}closo\text{-}2,1\text{-}MoCB_{10}H_9]$	violet	50	2012 vs, 1956 m, 1899 s	45.3 (45.9) [e]	5.5 (5.6)	1.7 (1.7)
9	$[1,2\text{-}\mu\text{-}NH_2\text{-}2,3\text{-}\mu\text{-}\{N(CH_2)_5\}\text{-}2,2\text{-}(CO)_2\text{-}2\text{-}I\text{-}closo\text{-}2,1\text{-}MoCB_{10}H_9]$	yellow	76	2069 s, 2027 s	19.0 (18.9)	4.1 (4.2)	5.3 (5.5)
10	$[1,2\text{-}\mu\text{-}NH_2\text{-}2,3\text{-}\mu\text{-}\{N(CH_2)_5\}\text{-}2,2\text{-}(CO)_2\text{-}2\text{-}Cl\text{-}closo\text{-}2,1\text{-}MoCB_{10}H_9]$	yellow	27	2081 s, 2038 s	22.9 (23.1)	5.1 (5.1)	6.7 (6.7)
11	$[1,2\text{-}\mu\text{-}NH_2\text{-}2,3\text{-}\mu\text{-}\{N(CH_2)_5\}\text{-}2\text{-}CO\text{-}2\text{-}I\text{-}2\text{-}PEt_3\text{-}closo\text{-}2,1\text{-}MoCB_{10}H_9]$	orange-red	58	1989 s	24.4 (24.6) [c]	5.4 (5.6)	4.1 (4.1)
12	$[1,2\text{-}\mu\text{-}NH_2\text{-}2,3\text{-}\mu\text{-}\{N(CH_2)_5\}\text{-}2\text{-}CO\text{-}2\text{-}Cl\text{-}2\text{-}PEt_3\text{-}closo\text{-}2,1\text{-}MoCB_{10}H_9]$	red-orange	60	1996 s	30.1 (30.1) [d]	7.0 (7.0)	5.3 (5.4)

[a] Measured in CH_2Cl_2; broad medium-intensity bands observed at *ca.* 2550 cm^{-1} in the spectra of all compounds are due to B–H absorptions. [b] Calculated values are given in parentheses. [c] Crystallizes with 1 mol equivalent of CH_2Cl_2. [d] Crystallizes with 0.25 mol equivalent of CH_2Cl_2. [e] Crystallizes with 1 mol equivalent of pentane.

in the presence of excess piperidine. The first step of this reaction is reasonably assumed to be the Me_3NO-assisted substitution of CO by $NH(CH_2)_5$ to directly give the $[N(PPh_3)_2]^+$ salt of intermediate **E** (Scheme 1). The subsequent reaction to give **3a** confirms that intermediate **E** can convert to **F** and supports the proposal that the α-B–H of the cage in **E** is sufficiently hydridic and the *N*-bound hydrogen of the coordinated piperidine sufficiently protonic that they can readily combine to eliminate H_2 and form the intramolecular piperidinyl bridge.

A similar H_2 elimination is also thought to occur in the reaction of **2a** with $Tl[PF_6]$ in the presence of piperidine, from which the new compound $[2,3\text{-}\mu\text{-}\{N(CH_2)_5\}\text{-}2,2,2\text{-}(CO)_3\text{-}6\text{-}NMe_3\text{-}closo\text{-}2,1\text{-}MoCB_{10}H_9]$ **5** was obtained. Compound **5** was characterized by the data in Tables 1–3. Consistent with the asymmetry of the cluster, the $^{11}B\{^1H\}$ NMR spectrum shows 10 separate resonances. Of these, two signals remain singlets in the proton-coupled ^{11}B NMR spectrum. These are attributed to the substituted boron atoms carrying NMe_3 or piperidinyl groups and are seen at δ 14.2 and 9.6. Peaks due to the piperidinyl group are also apparent in typical positions in the ^1H and $^{13}C\{^1H\}$ NMR spectra. A broad singlet diagnostic for the cage CH is observed in the ^1H NMR spectrum at δ 2.35 but, due to the compound's poor solubility, the corresponding broad resonance in the $^{13}C\{^1H\}$ NMR spectrum could not be observed.

Problems of solubility also frustrated attempts to obtain diffraction-quality crystals of **5** with a view to confirming its structure. However, it seems reasonable that the piperidinyl bridge in **5** would involve an α-boron atom in the C*B*BB*B* belt by analogy with compounds **3** and **4**. The formation of **5** presumably proceeds *via* $[2\text{-}\{NH(CH_2)_5\}\text{-}2,2,2\text{-}(CO)_3\text{-}6\text{-}NMe_3\text{-}closo\text{-}2,1\text{-}MoCB_{10}H_{10}]^-$ (**E′**), a B–NMe_3 substituted analogue of intermediate **E** (Scheme 1), and the final product **5** is a zwitterionic, B–NMe_3 substituted derivative of **F**. It is of interest to note that **E′** is an isomer of the species **C** in Scheme 1. However, whereas the C–NMe_3 bond in the latter appears unstable, the B–NMe_3 linkage in **E′** remains intact under these conditions, as we have observed previously.[6] Indeed, the observation that **5** can be formed by this synthetic route eliminates the possibility that the intermediate **C** (Scheme 1) undergoes a carbon-to-boron NMe_3 migration [6] and then displacement of the NMe_3 by formation of the piperidinyl bridge.

Piperidine has long been known as a potent reagent for the deboronation of carbaboranes.[8] There are also precedents for base degradation of carbametallaboranes.[1a,b] Although in the present systems the reagents and products are exposed to liberated piperidine during the reaction, we saw no evidence of species resulting from boron atom removal. However, the formation of cluster-degraded species cannot be excluded, as such products may simply be unstable. Indeed, such processes might even contribute to lowering of yields, particularly in those syntheses conducted at elevated temperatures.

Unlike compound **1a**, whose intramolecular nitrogen–molybdenum bond is easily broken in the presence of acids,[4] protonation of **3a** with $HBF_4{\cdot}OEt_2$ or HCl failed to lift the intramolecular N–Mo bond. In the case of **4**, the protonation probably occurred at the *C*–NH_2 nitrogen, and resulted only in decomposition and a mixture of unidentified products. However, the cations $\{M(PPh_3)\}^+$ (M = Cu, Ag), isolobal with the proton, were found readily to react with **3a** and **4** to form bimetallic complexes. Thus, treatment of **3a** or **4** with $[CuCl(PPh_3)]_4$ together with $Tl[PF_6]$ gave the heterobimetallic species $[2,7,11\text{-}\{Cu(PPh_3)\}\text{-}7,11\text{-}(\mu\text{-}H)_2\text{-}1\text{-}R\text{-}2,3\text{-}\mu\text{-}\{N(CH_2)_5\}\text{-}2,2,2\text{-}(CO)_3\text{-}closo\text{-}2,1\text{-}MoCB_{10}H_7]$ [R = H (**6**), NH_2 (**7**)] as the major products after column chromatography. The Ag analogue $[2,11\text{-}\{Ag(PPh_3)\}\text{-}11\text{-}\mu\text{-}H\text{-}2,3\text{-}\mu\text{-}\{N(CH_2)_5\}\text{-}2,2,2\text{-}(CO)_3\text{-}closo\text{-}2,1\text{-}MoCB_{10}H_9]$ **8** was similarly prepared from the reaction of **3a** with one equivalent each of $Ag[BF_4]$ and PPh_3.

Microanalytical, IR and NMR data for **6**–**8** are given in Tables 1–3. All these products form as violet crystals and have similar IR spectra in which the absorptions attributable to the

Table 2 ^{1}H and ^{13}C NMR data[a]

Compound	^{1}H δ[b]	^{13}C δ[c]
3a	7.67–7.27 (m, 30 H, Ph), 3.20–3.05 (m, 2 H, NCH_2), 2.88–2.67 (m, 2 H, NCH_2), 2.12 (br s, 1 H, cage CH), 1.83–1.27 (m, 6 H, CH_2)	238.8, 237.2, 227.1 (CO × 3), 134.1–126.8 (Ph), 59.3, 58.7 (NCH_2 × 2), 53.2 (br, cage C), 29.0, 28.4, 24.8 (CH_2 × 3)
4	7.67–7.24 (m, 30 H, Ph), 4.35 (m, 1 H, NCH_2), 3.40 (m, 2 H, NCH_2), 3.19 (m, 1 H, NCH_2), 2.00 (br s, 2 H, NH_2), 1.81–1.52 (m, 6 H, CH_2)	236.4, 235.6, 227.1 (CO × 3), 87.7 (br, cage C), 61.9, 54.2 (NCH_2 × 2), 29.6, 28.5, 25.1 (CH_2 × 3)
5	3.26–2.77 (m, 4 H, NCH_2), 2.87 (s, 9 H, Me), 2.35 (br s, 1 H, cage CH), 1.80–1.53 (m, 6 H, CH_2)	235.7, 233.3, 230.8 (CO × 3), 61.0, 60.7 (NCH_2 × 2), 58.1 (NMe_3), 29.1, 28.8, 24.3 (CH_2 × 3)
6	7.53–7.23 (m, 15 H, Ph), 3.11 (m, 2 H, NCH_2), 2.94 (m, 1H, NCH_2), 2.82 (m, 1H, NCH_2), 2.27 (br s, 1 H, cage CH), 1.83–1.54 (m, 6 H, CH_2)	224.9, 220.1, 217.8 (CO × 3), 134.2–129.5 (Ph), 61.0, 60.9 (NCH_2 × 2), 49.9 (br, cage C), 29.2 (CH_2 × 2), 24.4 (CH_2)
7	7.50–7.38 (m, 15 H, Ph), 5.02 (m, 1 H, NCH_2), 3.30–3.14 (m, 3 H, NCH_2), 2.37 (br s, 2 H, NH_2), 1.81 (m, 3 H, CH_2), 1.62 (m, 3 H, CH_2)	223.2, 218.5, 217.3 (CO × 3), 136.4–127.3 (Ph), 95.1 (br, cage C), 63.9, 55.4 (NCH_2 × 2), 30.0, 29.4, 24.7 (CH_2 × 3)
8	7.72–7.39 (m, 15 H, Ph), 3.15–2.22 (m, 4 H, NCH_2), 2.22 (br s, 1 H, cage CH), 1.80–1.56 (m, 6 H, CH_2)	219.9, 224.4, 228.0 (CO × 3), 136.4–128.8 (Ph), 60.8 (NCH_2 × 2), 49.3 (br, cage C), 29.3 (CH_2 × 2), 23.4 (CH_2)
9	3.30 (m, 1 H, NCH_2), 3.08–2.90 (m, 5 H, NH_2 and NCH_2), 1.88–1.50 (m, 6 H, CH_2)	204.8, 204.5 (CO × 2), 103.5 (br, cage C), 61.8, 49.7 (NCH_2 × 2), 29.5, 27.7, 24.0 (CH_2 × 3)
10	3.24 (m, 2 H, NCH_2), 3.04, 2.89 (br s × 2, 1 H × 2, NH × 2), *ca.* 2.90–2.77 (m, 2 H, NCH_2), 1.88–1.50 (m, 6 H, CH_2)	204.3, 203.4 (CO × 2), 106.9 (br, cage C), 61.0, 49.0 (NCH_2 × 2), 29.1, 27.3, 24.0 (CH_2 × 3)
11	5.30, 3.21, 2.93, 2.86 (m × 4, 1 H × 4, NCH_2), 2.64, 2.37 (br s × 2, 1 H × 2, NH × 2), 2.13–1.92 [dq × 3, J(PH) = *ca.* 7, 2 H × 3, PCH_2 × 3], 1.81–1.47 (m, 6 H, CH_2), 1.13 [dt, J(PH) = 15, J(HH) = 7, 9 H, CH_3]	219.9 [d, CO, J(PC) = 12], 100.6 (br, cage C), 62.2, 48.5 (NCH_2 × 2), 29.8, 27.4, 24.3 (CH_2 × 3), 19.9 [d, PCH_2, J(PC) = 26], 8.9 (br, CH_3)
12	5.30, 3.18, 3.05 (m × 3, 1 H × 3, NCH_2), 2.65 (m, 2 H, NCH_2 and NH), 2.40 (br s, 1 H, NH), 2.10–1.78 [dq × 3, J(PH) = *ca.* 7, 2 H × 3, PCH_2 × 3], 1.72–1.43 (m, 6 H, CH_2), 1.12 [dt, J(PH) = 15, J(HH) = 7, 9 H, CH_3]	220.0 [d, CO, J(PC) = 12], 104.3 (br, cage C), 60.7, 47.7 (NCH_2 × 2), 29.5, 27.1, 24.2 (CH_2 × 3), 16.9 [d, PCH_2, J(PC) = 25], 8.2 [d, CH_3, J(PC) = 4]

[a] Chemical shifts (δ) in ppm, coupling constants (J) in Hz, measurements at ambient temperatures in CD_2Cl_2. [b] Resonances for terminal BH protons occur as broad unresolved signals in the range δ *ca.* −1 to +3. [c] ^{1}H-decoupled chemical shifts are positive to high frequency of $SiMe_4$.

Table 3 ^{11}B and ^{31}P NMR data[a]

Compound	^{11}B δ[b]	^{31}P δ[c]
3a	9.9 [B(3)],[d] 5.4, 1.4, 1.2, −5.0, −5.6, −13.3, −18.0, −18.8 (2 B)	21.7
4	12.6 [B(3)], 0.9, −1.8 (2 B), −3.3, −10.5, −11.4, −11.8, −16.4, −17.7	21.7
5	14.2,[e] 9.6,[e] 4.7, 0.6, −1.5, −2.2, −13.4, −17.7, −18.4, −19.3	–
6	10.3 (2 B),[f] −2.5, −6.4, −8.1, −11.5, −12.1, −14.4, −16.3 (2 B)	10.3 (br)
7	12.7 [B(3)], 5.1, −2.1, −6.0, −10.3, −11.5, −12.5, −13.1, −14.9, −15.5	10.2 (br)
8	9.8 (2 B),[f] −3.3, −7.2 (2 B), −9.1, −11.1, −15.5 (3 B)	18.4 [br d × 2, J(^{109}AgP) = 650, J(^{107}AgP) = 570]
9	14.9 [B(3)], 12.3, 10.9, 4.8, 0.1, −6.5, −8.9, −10.6, −12.9, −23.3	–
10	15.5 [B(3)], 11.5, 11.0, 6.2, 0.9, −6.9, −9.0, −11.0, −12.7, −23.0	–
11	12.5 [B(3)], 9.1, 8.2, 3.4, −0.9, −8.8, −10.4, −13.3, −15.0, −24.1	14.9
12	13.2 [B(3)], 9.6, 6.7, 4.3, −0.2, −9.5, −10.7, −13.5, −14.6, −24.1	23.2

[a] Chemical shifts (δ) in ppm, coupling constants (J) in Hz, measurements at ambient temperatures in CD_2Cl_2. [b] ^{1}H-decoupled chemical shifts are positive to high frequency of $BF_3{\cdot}Et_2O$ (external); peaks are of unit integral except where indicated. [c] ^{1}H-decoupled chemical shifts are positive to high frequency of 85% H_3PO_4 (external). [d] The α-boron atom carrying the piperidinyl substituent. [e] The α-boron atom carrying the piperidinyl or trimethylamine substituents. [f] The peak due to B(3) coincides with that of another, non-substituted boron.

CO ligands move to high frequency compared with those of the precursors **3a** and **4**. Their ^{1}H NMR spectra reveal diagnostic resonances for the cage CH at δ 2.27 for **6** and 2.22 for **8**, whilst the NH_2 protons in **7** resonate at δ 2.37. No indications were observed in the ^{1}H NMR spectra of compounds **6**–**8** that may be attributed to the H atoms involved in the B–H⟶M interactions. This is likely due to fluxionality of the $\{M(PPh_3)\}^+$ fragments over the cage surface that is fast on the NMR time scale.[9] In the $^{13}C\{^{1}H\}$ NMR spectra, there are also very broad resonances corresponding to the cage-carbon atoms at δ 49.9 (**6**) and 49.3 (**8**), and at δ 95.1 for **7**. The $^{31}P\{^{1}H\}$ NMR spectra show simple resonances with a broad peak at δ 10.3 for **6** and 10.2 for **7**, and a pair of broad doublets centered at δ 18.4 for **8**, the latter with typical ^{107}Ag–^{31}P and ^{109}Ag–^{31}P couplings of 570 and 650 Hz, respectively.[10]

The dynamic behaviour of **6**–**8** in solution means that the NMR data are insufficient to establish whether the copper or silver fragments are located on the side of the cage without any direct Mo–M interaction or whether a Mo–M bond is present in the solid state structure. In order to establish the exact mode of attachment of the $\{M(PPh_3)\}^+$ groups to the molybdenacarbaborane cage, a single-crystal X-ray diffraction study was undertaken for compound **6**. The molecular structure of **6** is shown in Fig. 2. It is immediately apparent that there is a bond between the Mo and Cu atoms [Mo–Cu = 2.7697(12) Å]. This Mo–Cu interaction is further supported by two three-centre two-electron B–H⟶Cu bonds [Cu–B(3) = 2.183(9) and Cu–B(4) = 2.181(9) Å]. It is interesting to compare the structure of **6** with that of the related species [7,8,12-{$Cu(PPh_3)$}-7,8,12-(μ-H)$_3$-2,2,2-(CO)$_3$-2-PPh_3-*closo*-2,1-$MoCB_{10}H_8$], prepared similarly from the anion [2,2,2-(CO)$_3$-2-PPh_3-*closo*-2,1-$MoCB_{10}H_{11}]^-$, in which the $\{Cu(PPh_3)\}^+$ fragment is attached exopolyhedrally to the cage framework by three B–H⟶Cu linkages with no direct Mo–Cu bond.[9] On the basis of a preliminary (heavy atom) X-ray diffraction study, compound **7** is known to have a molecular structure similar to **6**, perhaps surprisingly without any interaction between Cu and the pendant NH_2 group. An X-ray diffraction study for **8** could not be performed primarily as its instability in solution frustrated attempts to obtain suitable crystals. However, its structure is

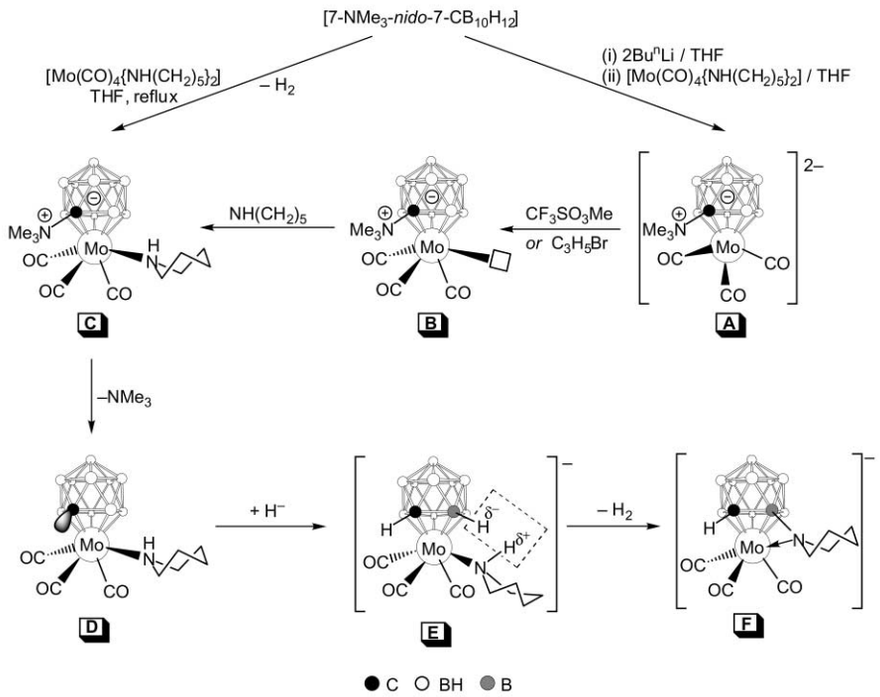

Scheme 1 Proposed pathway for the formation of the anion of **3**.

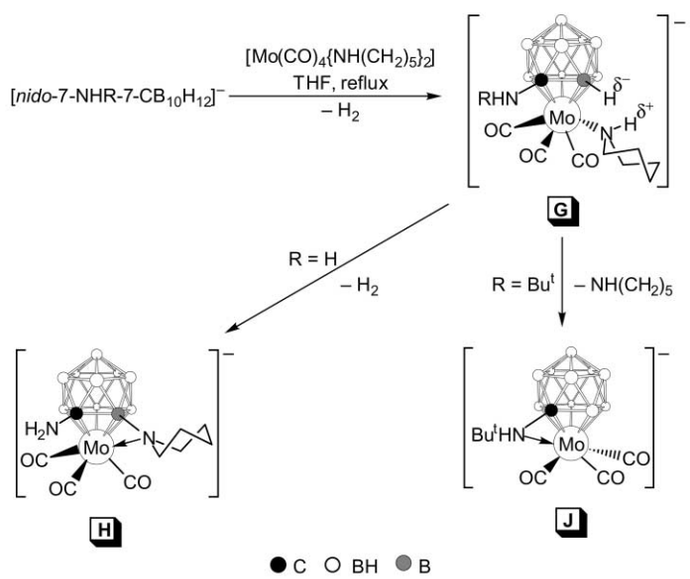

Scheme 2 Proposed pathway for the formation of the anions of **4** and **1a**.

reasonably assumed to be similar to that of **6**, except that there is only one B–H⟶Ag agostic bond. This is by analogy with several related compounds, in which the exopolyhedral silver atom only requires three coordination.[9,11] In **8**, there are two non-equivalent β-boron atoms in the CB*BB*B ring bonded to molybdenum, and either of these could be involved in the B–H⟶Ag linkage. Steric considerations suggest that the β-boron atom most distant from the piperidinyl group would be chosen: that is, compound **8** would be the 2,11-{Ag(PPh_3)} isomer, as depicted here. However, the alternative, 2,7- isomer cannot be ruled out without a structural study; indeed, it is possible that both isomers are involved in the solution dynamic processes.

In earlier work, we have investigated oxidation reactions of monoanionic molybdenacarbaboranes including [$N(PPh_3)_2$]-[2,2,2,2-$(CO)_4$-*closo*-2,1-$MoCB_{10}H_{11}$] or **1a**.[4–7] These reactions afford Mo^{IV} complexes in which the trianionic carbaborane ligand helps stabilize the high oxidation state. Following a similar strategy, treatment of **4** with I_2 in THF gave the Mo^{IV} complex [1,2-μ-NH_2-2,3-μ-{$N(CH_2)_5$}-2,2-$(CO)_2$-2-I-*closo*-2,1-$MoCB_{10}H_9$] **9**. The corresponding chloride compound **10** was prepared by treating **4** with *N*-chlorosuccinimide or tris(4-bromophenyl)aminium hexachloroantimonate. In the case of the latter reagent, the yield was very poor. Compounds **9** and **10** are characterized by the data given in Tables 1–3. Ten resonances are seen in each of the $^{11}B\{^1H\}$ NMR spectra, of which the signals at δ 14.9 (**9**) and 15.5 (**10**) are due to the piperidinyl-substituted boron as the remaining signals all appear as doublets in the fully coupled ^{11}B NMR spectra. In the ^1H NMR spectrum of compound **10**, the NH_2 protons are seen to be inequivalent, giving rise to two broad peaks at δ 2.89 and 3.04. For compound **9**, signals for these protons cannot be observed, due to overlap with those for the piperidinyl methylene groups. The $^{13}C\{^1H\}$ spectra of **9** and **10** show characteristic broad

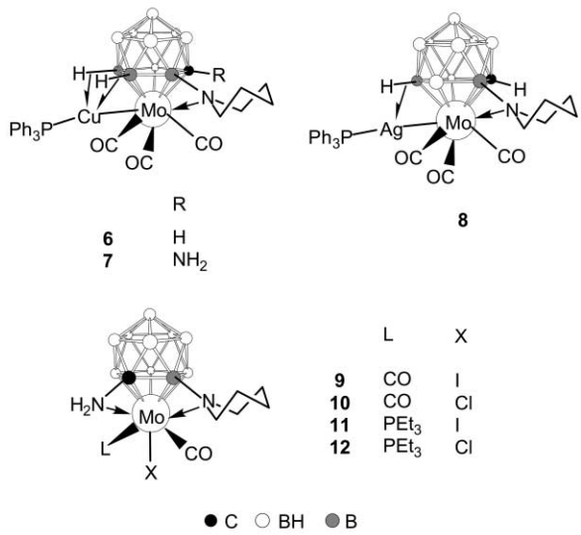

Chart 2

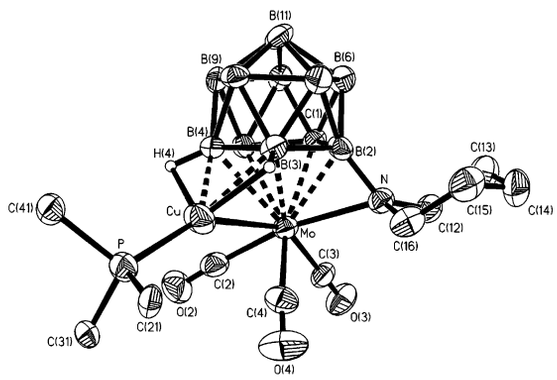

Fig. 2 Structure of **6** showing the crystallographic labeling scheme. Hydrogen atoms, except H(3) and H(4), are omitted and thermal ellipsoids are drawn at the 40% probability level. Selected bond lengths (Å) and angles (°): Mo–Cu 2.7697(12), Mo–N 2.300(6), Mo–C(1) 2.341(7), Mo–C(2) 2.007(9), Mo–C(3) 2.026(8), Mo–C(4) 1.987(9), Mo–B(2) 2.209(8), Mo–B(3) 2.403(8), Mo–B(4) 2.460(8), Mo–B(5) 2.399(8), B(3)–Cu 2.183(9), B(4)–Cu 2.181(9), Cu–P 2.180(2), B(2)–N 1.464(9); C(2)–Mo–N 168.2(2), C(3)–Mo–N 88.4(3), C(4)–Mo–N 91.9(3), N–Mo–C(1) 70.0(2), B(2)–N–Mo 67.7(4), N–Mo–Cu 109.2(2), P–Cu–B(4) 142.6(2), P–Cu–B(3) 150.6(3).

resonances for the cage-carbon at δ 103.5 (**9**) and 106.9 (**10**), shifted to lower field compared with that in the precursor **4** (δ 87.7). This low-field shift in such systems is diagnostic of amino groups forming an intramolecular bridge and suggested that the cluster-bound NH_2 group was now also bonded to the molybdenum. The non-equivalence observed for the NH_2 protons in **10** is also consistent with such a feature. However, to confirm the presence of an intramolecular NH_2 bridge, an X-ray diffraction study for **9** was carried out.

The molecular structure of **9** is shown in Fig. 3. This determination confirms that during the oxidation reaction, the intramolecular piperidinyl bridge remains intact while the NH_2 group forms a new intramolecular bond to the Mo atom. In addition, the molybdenum centre is also bonded to the open face of the carbaborane moiety and on the other side to two linear CO ligands and an iodide. Compared to other boron atoms in the same $\overline{CBBBB}$ belt, B(2) has the shortest interaction with the Mo atom [Mo–B(2) = 2.207(11) Å *versus* Mo–B(3) = 2.402(11), Mo–B(4) = 2.462(12) and Mo–B(5) = 2.372(11) Å]. Similarly, the bond length Mo–C(1) [2.141(8) Å] is much shorter than that [2.437(6) Å] in the related Mo^{IV} complex [2,2,2,2-$(CNBu^t)_4$-2-I-*closo*-2,1-$MoCB_{10}H_{11}$].[5] Compound **9** again shows slippage of molybdenum towards the side of the

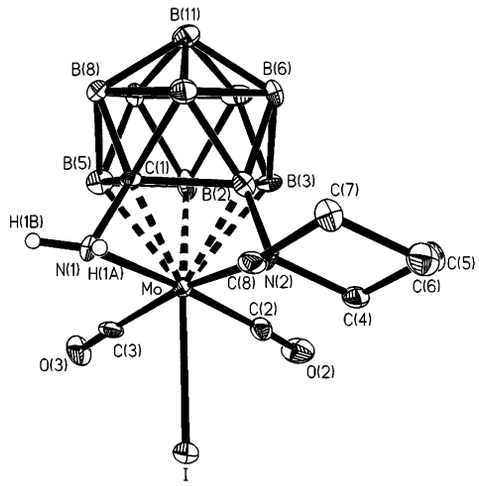

Fig. 3 Structure of **9** showing the crystallographic labeling scheme. Hydrogen atoms, except H(1A) and H(1B), are omitted and thermal ellipsoids are drawn at the 40% probability level. Selected bond lengths (Å) and angles (°): Mo–C(2) 2.047(10), Mo–C(3) 2.065(12), Mo–C(1) 2.141(8), Mo–B(2) 2.207(11), Mo–N(1) 2.249(8), Mo–N(2) 2.326(7), Mo–B(5) 2.372(11), Mo–B(3) 2.402(11), Mo–B(4) 2.462(12), Mo–I 2.7542(10), C(1)–N(1) 1.441(11), B(2)–N(2) 1.440(13); C(1)–Mo–N(1) 38.2(3), C(2)–Mo–N(1) 174.4(3), C(3)–Mo–N(1) 101.0(3), C(1)–Mo–N(2) 74.6(3), C(2)–Mo–N(2) 99.7(3), C(3)–Mo–N(2) 170.3(3), B(2)–Mo–N(1) 75.2(3), B(2)–Mo–N(2) 36.9(3), N(1)–Mo–N(2) 78.1(3), N(1)–Mo–I 95.4(2), N(2)–Mo–I 88.8(2), C(1)–Mo–I 132.5(2), C(2)–Mo–I 79.3(3), C(3)–Mo–I 81.6(3).

cage where the intramolecular linkages are formed. Although the angles at the two intramolecular bridges are essentially the same [Mo–N(1)–C(1) = 66.8(4) and Mo–N(2)–B(2) = 67.0(5)°], the bond distances between Mo and the N atoms are quite different [Mo–N(1) = 2.249(8) and Mo–N(2) = 2.326(7) Å]. Overall, the [7-NH_2-8-{$N(CH_2)_5$}-*nido*-7-$CB_{10}H_9$]$^{3-}$ fragment in **9** formally donates *ten* electrons to the Mo^{IV} centre. As far as we are aware, such a ($6\pi + 2 \times 2\sigma$) bonding mode for a cage system in metallacarbaborane chemistry has not previously been seen.

On heating with PEt_3 in CH_2Cl_2 for 40 h, compound **9** reacts to form a mixture of two products. Separation of the mixture by preparative thin-layer chromatography afforded the compounds [1,2-μ-NH_2-2,3-μ-{$N(CH_2)_5$}-2-CO-2-X-2-PEt_3-*closo*-2,1-$MoCB_{10}H_9$] [X = I (**11**), Cl (**12**)] which were both characterized by the IR, NMR and microanalytical data listed in Tables 1–3. In their IR spectra, there is only one CO stretching band at 1989 cm^{-1} for **11** and 1996 cm^{-1} for **12**, confirming that the substitution reaction has occurred. Their $^{11}B\{^1H\}$ NMR spectra are very similar to those of the parent species **9** and **10**, and in their ^1H NMR spectra the NH_2 protons give rise to two separate broad signals at δ 2.64 and 2.37 for **11** and δ 2.65 and 2.40 for **12**, to be compared with those at δ 3.04 and 2.89 for **10**. Each of the $^{13}C\{^1H\}$ NMR spectra display only one phosphorus-coupled doublet [J(PC) = 12 Hz] for the CO ligand at δ 219.9 for **11** and δ 220.0 for **12**. Similar to those of complexes **9** and **10**, the signals for the cage-carbons are observed to lower field, at δ 100.6 (**11**) and δ 104.3 (**12**), again indicating the presence of H_2N–Mo intramolecular bonds. The signals due to the PEt_3 ligand in the $^{31}P\{^1H\}$ NMR spectra are observed at δ 14.9 for **11** and δ 23.2 for **12**.

Interestingly, it appears at first sight that neither of the intramolecular linkages in **9** (or **10**) is displaced by PEt_3, even at elevated temperatures. Indeed, the piperidinyl bridge in **4** was noted to be similarly unaffected under the same conditions. This contrasts with the behaviour of **1a**, whose μ-$NHBu^t$ unit is readily lifted by addition of PEt_3 at room temperature.[4] However, it may be speculated that the CO substitution in the present system involves an initial lifting of one of the amino bridges, allowing attachment of PEt_3 to the Mo centre, followed

by regeneration of the intramolecular donor bond and displacement of CO. It is notable that – regardless of the manner of CO replacement – the products **11** and **12** are formed as single isomers, despite there being two non-equivalent CO groups in the parents **9** and **10**.

It may further be suggested that formation of **12** occurs *via* replacement of the iodide in the starting material **9** by chloride from the CH_2Cl_2 solvent and then CO substitution by PEt_3. Indeed, when the same reaction was carried out in refluxing THF, only **11** was isolated after 6 h. Furthermore, complex **12** likewise could independently be obtained from **10** and PEt_3 in THF. Compound **9**, when refluxed with PEt_3 in $CHCl_3$, gave only **11** after 8 h: extended reaction times did not result in conversion to compound **12** but instead increased decomposition. Evidently at these elevated temperatures **9** reacts with PEt_3 to give **11** much more rapidly than it can react with $CHCl_3$; and once **11** is formed, it cannot be converted to **12** in the chlorinated solvent.

Conclusion

Two novel anionic molybdenum-monocarbaborane complexes **3** and **4** have been synthesized. Both contain an intramolecular donor bond to the molybdenum centre originating from a piperidinyl group that is also anchored to the carbaborane. The formation of the intramolecular bridge by elimination (as H_2) of a proton from a metal-bound ligand plus a hydride from a cage boron atom may point to a more general route to linkages of this type, including donor atoms other than nitrogen. Treatment of the anions of **3** or **4** with $\{M(PPh_3)\}^+$ gives rise to bimetallic products **6**–**8** with direct metal–metal bonds. Oxidation of **4** gave access to several novel Mo^{IV} compounds **9**–**12** in which, overall, the carbaborane ligand bearing two amino substituents formally acts as a 10-electron donor ($6\pi + 2 \times 2\sigma$) to the Mo atom. To our knowledge, this donor mode is unprecedented in metallacarbaborane chemistry and such ligands would certainly prove useful in stabilizing other high-oxidation state metal centres.

Experimental

General

All reactions were carried out under an atmosphere of dry, oxygen-free nitrogen using standard Schlenk line techniques. Solvents were stored over and distilled from appropriate drying agents under nitrogen prior to use. Petroleum ether here refers to that fraction of boiling point 40–60 °C. Chromatography columns (typically *ca.* 15 cm in length and *ca.* 2 cm in diameter) were packed with silica gel (Acros, 60–200 mesh). Purification of products by column chromatography usually resulted in elution of only a single band containing the desired product. However, as is typical in such procedures some coloured material remained at the top of the column, failing to elute. Preparative thin-layer chromatography (TLC) was performed on Uniplates (silica gel G, Analtech). NMR spectra were recorded at the following frequencies: ^{1}H 360.1, ^{13}C 90.6, ^{11}B 115.5 and ^{31}P 145.8 MHz. The complexes $[CuCl(PPh_3)]_4$,[12] $[N(PPh_3)_2][2,2,2,2\text{-}(CO)_4\text{-}closo\text{-}2,1\text{-}MoCB_{10}H_{11}]$[2d] and **2a**,[6] and the carbaboranes 7-NH_3-*nido*-7-$CB_{10}H_{12}$,[13] 7-NMe_3-*nido*-7-$CB_{10}H_{12}$[14] and 7-NH_2Bu^t-*nido*-7-$CB_{10}H_{12}$[15] were prepared according to the literature. The $[NHMe_3]^+$ and $[N(PPh_3)_2]^+$ salts of [*nido*-7-$CB_{10}H_{13}]^-$ were synthesized by methods similar to that of Knoth *et al.*[13] and $[FeI(CO)_2(\eta\text{-}C_5Me_5)]$ was prepared from $[Fe(CO)_2(\eta\text{-}C_5Me_5)]_2$.[16] All other materials were used as received.

Syntheses

$[N(PPh_3)_2][2,3\text{-}\mu\text{-}\{N(CH_2)_5\}\text{-}2,2,2\text{-}(CO)_3\text{-}closo\text{-}2,1\text{-}MoCB_{10}H_{10}]$. *Method (i).* The reagent Bu^nLi (1 cm^3, 2.5 M solution in hexanes, 2.50 mmol) was added to a THF (30 cm^3) solution of the carbaborane 7-NMe_3-*nido*-7-$CB_{10}H_{12}$ (0.24 g, 1.25 mmol) at *ca.* −78 °C. The resultant suspension was stirred as it warmed to *ca.* −40 °C over 10 min, and solid $[Mo(CO)_4\{NH(CH_2)_5\}_2]$ (0.47 g, 1.24 mmol) was added. After stirring for 3 h, the mixture was treated with CF_3SO_3Me (0.15 cm^3, 1.33 mmol) and stirring continued for 1 h. $[N(PPh_3)_2]Cl$ (0.72 g, 1.25 mmol) was added and the resulting mixture stirred overnight. After filtration through a Celite plug, the solvent was removed *in vacuo.* The residue was taken up in CH_2Cl_2 (2 cm^3) and the solution chromatographed. A pink fraction was eluted with neat CH_2Cl_2. After removal of the solvent, the residue was extracted with Et_2O (3 × 50 cm^3) and the extract filtered and evaporated *in vacuo* to give pink microcrystals of $[N(PPh_3)_2][2,3\text{-}\mu\text{-}\{N(CH_2)_5\}\text{-}2,2,2\text{-}(CO)_3\text{-}closo\text{-}2,1\text{-}MoCB_{10}H_{10}]$ **3a** (0.15 g, 13%).

Method (ii). An identical procedure to that above, except that $CH_2{=}CHCH_2Br$ (0.12 cm^3, 1.39 mmol) was used instead of CF_3SO_3Me, also yielded **3a** (0.14 g, 12%).

Method (iii). A mixture of 7-NMe_3-*nido*-7-$CB_{10}H_{12}$ and $[Mo(CO)_4\{NH(CH_2)_5\}_2]$ was heated to reflux in THF for 12 h. After addition of $[N(PPh_3)_2]Cl$ and column chromatography as above, compound **3a** was obtained in poor yield (*ca.* 6%). Likewise, with [X][*nido*-7-$CB_{10}H_{13}$] [X = $NHMe_3$, $N(PPh_3)_2$] as the carbaborane reagent under the same conditions, the same product was also formed albeit at yet lower yields (4–5%).

Method (iv). The complex $[N(PPh_3)_2][2,2,2,2\text{-}(CO)_4\text{-}closo\text{-}2,1\text{-}MoCB_{10}H_{11}]$ (0.10 g, 0.15 mmol) was dissolved in CH_2Cl_2 (10 cm^3) and $NH(CH_2)_5$ (*ca.* 0.10 cm^3) was added. This solution was treated with Me_3NO (*ca.* 0.50 g, 0.67 mmol) in several portions over 24 h until all the starting material had been consumed (monitored by IR spectroscopy). The reaction mixture was worked up as described above to give **3a** (0.06 g).

$[Fe(CO)_3(\eta\text{-}C_5Me_5)][2,3\text{-}\mu\text{-}\{N(CH_2)_5\}\text{-}2,2,2\text{-}(CO)_3\text{-}closo\text{-}2,1\text{-}MoCB_{10}H_{10}]$. The complex $[FeI(CO)_2(\eta\text{-}C_5Me_5)]$ (0.08 g, 0.21 mmol) was dissolved in THF (10 cm^3), and $Ag[BF_4]$ (0.042 g, 2.20 mmol) added. The mixture was stirred for 30 min, filtered through Celite, and the filtrate evaporated *in vacuo.* Compound **3a** (0.20 g, 0.22 mmol) was combined with this residue in CH_2Cl_2 (20 cm^3) and the mixture stirred overnight. The solution was concentrated to *ca.* 1 cm^3 by evaporation *in vacuo* and chromatographed, eluting with CH_2Cl_2–petroleum ether (2 : 1). A brown-red fraction was collected which afforded $[Fe(CO)_3(\eta\text{-}C_5Me_5)][2,3\text{-}\mu\text{-}\{N(CH_2)_5\}\text{-}2,2,2\text{-}(CO)_3\text{-}closo\text{-}2,1\text{-}MoCB_{10}H_{10}]$ **3b** (0.05 g, 35%). IR: ν_{max}(CO): 2077 m, 2043 m, 2006 vs, 1968 w, 1939 w, 1891 s cm^{-1}. Compound **3b** was identified by NMR spectroscopy and by an X-ray diffraction study.

$[N(PPh_3)_2][1\text{-}NH_2\text{-}2,3\text{-}\mu\text{-}\{N(CH_2)_5\}\text{-}2,2,2\text{-}(CO)_3\text{-}closo\text{-}2,1\text{-}MoCB_{10}H_9]$. The carbaborane 7-$NH_3$-*nido*-7-$CB_{10}H_{12}$ (0.50 g, 3.35 mmol) was dissolved in THF (30 cm^3) and the solution cooled to 0 °C and treated with Bu^nLi (1.4 cm^3, 3.50 mmol). The resultant was stirred for 30 min with warming to room temperature. Solid $[Mo(CO)_4\{NH(CH_2)_5\}_2]$ (1.27 g, 3.36 mmol) was introduced to the mixture and this then was heated to reflux for 6 h. After cooling to ambient temperatures, $[N(PPh_3)_2]Cl$ (1.93 g, 3.36 mmol) was added and stirring continued for a further 1 h. Evaporation *in vacuo* afforded a red-brown residue which was subjected to rapid column chromatography. Elution with CH_2Cl_2 gave a violet band which was collected and evaporated *in vacuo* to give violet microcrystalline $[N(PPh_3)_2][1\text{-}NH_2\text{-}2,3\text{-}\mu\text{-}\{N(CH_2)_5\}\text{-}2,2,2\text{-}(CO)_3\text{-}closo\text{-}2,1\text{-}MoCB_{10}H_9]$ **4** (0.78 g).

$[2,3\text{-}\mu\text{-}\{N(CH_2)_5\}\text{-}2,2,2\text{-}(CO)_3\text{-}6\text{-}NMe_3\text{-}closo\text{-}2,1\text{-}MoCB_{10}H_9]$. To a CH_2Cl_2 (20 cm^3) solution of **2a** (0.20 g, 0.20 mmol) was added $NH(CH_2)_5$ (*ca.* 0.05 cm^3) followed by $Tl[PF_6]$ (0.07 g, 0.20 mmol). The mixture was stirred overnight. After removal of solvent *in vacuo*, the residue was chromatographed. Elution

Table 4 Data for crystal structure analyses of compounds **3b**, **6**·CH_2Cl_2 and **9**

	3b	**6**·CH_2Cl_2	**9**
Chemical formula	$C_{22}H_{35}B_{10}FeMoNO_6$	$C_{28}H_{37}B_{10}Cl_2CuMoNO_3P$	$C_8H_{21}B_{10}IMoN_2O_2$
M	669.40	805.04	508.21
Crystal system	Monoclinic	Monoclinic	Orthorhombic
Space group	$P2_1$	$P2_1/c$	$Pbca$
a/Å	9.346(2)	13.827(2)	15.322(2)
b/Å	18.006(3)	15.0408(13)	14.112(5)
c/Å	18.339(3)	18.274(2)	16.893(3)
β/°	90.94(2)	107.015(10)	
Z	4	4	8
U/Å^3	3085.7(10)	3634.1(7)	3653(2)
μ(Mo-Kα)/cm^{-1}	9.13	11.53	24.10
T/K	293	293	173
Reflections measured	6443	6588	3930
Independent reflections	5728	4745	3226
R_{int}	0.0580	0.0790	0.0539
$wR2$ (all data), $R1$ [a]	0.1375, 0.0650 [b]	0.0982, 0.0541	0.1177, 0.0546

[a] $F_o > 4\sigma(F_o)$. [b] Flack parameter = −0.11(5).

with CH_2Cl_2–petroleum ether (2 : 1) removed a violet band from which [2,3-μ-{$N(CH_2)_5$}-2,2,2-$(CO)_3$-6-NMe_3-*closo*-2,1-$MoCB_{10}H_9$] **5** (0.05 g) was obtained as a violet solid.

[2,7,11-{Cu(PPh_3)}-7,11-(μ-H)$_2$-1-R-2,3-μ-{$N(CH_2)_5$}-2,2,2-$(CO)_3$-*closo*-2,1-$MoCB_{10}H_7$] (R = H, NH_2). The compounds **3a** (0.15 g, 0.16 mmol), [CuCl(PPh_3)]$_4$ (0.064 g, 0.04 mmol) and Tl[PF_6] (0.062 g, 0.18 mmol) were treated with CH_2Cl_2 (20 cm^3) and the mixture stirred overnight. The suspension was filtered through Celite, and solvent was then removed *in vacuo*. The residue was chromatographed, eluting with CH_2Cl_2–light petroleum (1 : 1). A violet fraction was collected and evaporated *in vacuo* to give [2,7,11-{Cu(PPh_3)}-7,11-(μ-H)$_2$-2,3-μ-{$N(CH_2)_5$}-2,2,2-$(CO)_3$-*closo*-2,1-$MoCB_{10}H_8$] **6** (0.067 g) as violet microcrystals.

Similarly, compound **4** (0.10 g, 0.11 mmol), [CuCl(PPh_3)]$_4$ (0.037 g, 0.03 mmol) and Tl[PF_6] (0.039 g, 0.11 mmol) in THF gave [2,7,11-{Cu(PPh_3)}-7,11-(μ-H)$_2$-1-NH_2-2,3-μ-{$N(CH_2)_5$}-2,2,2-$(CO)_3$-*closo*-2,1-$MoCB_{10}H_7$] **7** (0.043 g) as violet prisms after column chromatography with CH_2Cl_2–petroleum ether (6 : 5).

[2,11-{Ag(PPh_3)}-11-μ-H-2,3-μ-{$N(CH_2)_5$}-2,2,2-$(CO)_3$-*closo*-2,1-$MoCB_{10}H_9$]. Compound **3a** (0.24 g, 0.26 mmol) was added to PPh_3 (0.066 g, 0.25 mmol) and Ag[BF_4] (0.05 g, 0.26 mmol) in CH_2Cl_2 (20 cm^3) and the resulting mixture stirred for 2 h. After filtration through Celite, solvent was removed *in vacuo*. The residue was taken up in CH_2Cl_2 (*ca.* 2 cm^3) and chromatographed. Elution with CH_2Cl_2–light petroleum (2 : 1) removed a violet fraction from which [2,11-{Ag(PPh_3)}-11-μ-H-2,3-μ-{$N(CH_2)_5$}-2,2,2-$(CO)_3$-*closo*-2,1-$MoCB_{10}H_9$] **8** (0.097 g) was obtained.

[1,2-μ-NH_2-2,3-μ-{$N(CH_2)_5$}-2,2-$(CO)_2$-2-X-*closo*-2,1-$MoCB_{10}H_9$] (X = I, Cl). A THF (20 cm^3) solution of **4** (0.10 g, 0.11 mmol) was cooled to 0 °C and solid I_2 (0.027 g, 0.11 mmol) added. The mixture was allowed to warm to room temperature and stirring continued for 6 h, during which time the solution changed colour from violet to dark yellow. Solvent was removed *in vacuo* and the residue was chromatographed, elution with CH_2Cl_2–petroleum ether (3 : 2) giving a yellow fraction. The latter was collected and evaporated *in vacuo* to give yellow microcrystals of [1,2-μ-NH_2-2,3-μ-{$N(CH_2)_5$}-2,2-$(CO)_2$-2-I-*closo*-2,1-$MoCB_{10}H_9$] **9** (0.041 g).

Similarly, compound **4** (0.10 g, 0.11 mmol) and *N*-chlorosuccinimide (0.029 g, 0.22 mmol) gave [1,2-μ-NH_2-2,3-μ-{$N(CH_2)_5$}-2,2-$(CO)_2$-2-Cl-*closo*-2,1-$MoCB_{10}H_9$] **10** (0.012 g) as yellow crystals, after chromatography (CH_2Cl_2 eluant) and crystallization from CH_2Cl_2–petroleum ether (−30 °C).

[1,2-μ-NH_2-2,3-μ-{$N(CH_2)_5$}-2-CO-2-X-2-PEt_3-*closo*-2,1-$MoCB_{10}H_9$] (X = Cl, I). *Method (i)*. Compound **9** (0.050 g, 0.10 mmol) was treated with PEt_3 (0.03 cm^3, 0.20 mmol) in refluxing CH_2Cl_2 (20 cm^3) for 40 h. The resultant solution was concentrated to *ca.* 1 cm^3 by evaporation *in vacuo* and purified by column chromatography, eluting with CH_2Cl_2–petroleum ether (2 : 1). The red-orange fraction so obtained was found by qualitative TLC to be a mixture of two very similar compounds. Preparative TLC of this mixture, eluting with CH_2Cl_2–petroleum ether (8 : 3) gave three separate bands. Upon recrystallization from CH_2Cl_2–petroleum ether, the first two fractions gave microcrystals of, respectively, orange-red [1,2-μ-NH_2-2,3-μ-{$N(CH_2)_5$}-2-CO-2-I-2-PEt_3-*closo*-2,1-$MoCB_{10}H_9$] **11** (0.018 g, 31%, R_f 0.65) and red-orange [1,2-μ-NH_2-2,3-μ-{$N(CH_2)_5$}-2-CO-2-Cl-2-PEt_3-*closo*-2,1-$MoCB_{10}H_9$] **12** (0.014 g, 28%, R_f 0.55). The third fraction was identified (IR and $^{11}B\{^1H\}$ NMR spectroscopy) as unreacted **9** (*ca.* 0.001 g, R_f 0.45).

Method (ii). Alternatively, a solution of **9** (0.050 g, 0.10 mmol) in THF (20 cm^3) was heated to reflux with PEt_3 (0.1 cm^3) for 6 h. Volatiles were removed *in vacuo* and the residue redissolved in the minimum (*ca.* 1 cm^3) of CH_2Cl_2 and transferred to the top of a chromatography column. Elution with CH_2Cl_2–petroleum ether (1 : 1) gave a red-orange fraction that was collected and evaporated to give microcrystalline **11** (0.034 g).

Method (iii). By a similar procedure, **10** (0.015 g, 0.04 mmol) and PEt_3 (0.04 cm^3) after chromatography (CH_2Cl_2–petroleum ether, 8 : 3) and recrystallization, yielded microcrystals of **12** (0.011 g).

Crystallography

Experimental data for compounds **3b**, **6** and **9** are recorded in Table 4. Diffracted intensities were collected on an Enraf-Nonius CAD4 diffractometer using Mo-Kα X-radiation (λ = 0.71073 Å). Final unit cell dimensions were determined from the setting angles of 25 accurately centered reflections. Intensity data were corrected for Lorentz and polarization effects after which semi-empirical absorption corrections were applied.

All structures were solved with conventional direct methods and refined by full-matrix least-squares on all F^2 data using SHELXTL version 5.03 and SHELXL-97.[17,18] All non-hydrogen atoms were assigned anisotropic thermal displacement parameters. The locations of the cage-carbon atoms were verified by examination of the appropriate internuclear distances in conjunction with the magnitudes of their isotropic thermal displacement parameters. The agostic B–H⟶Cu hydrogens H(3) and H(4) in **6**, along with hydrogens H(1a) and H(1b) in **9**, were

located in difference Fourier syntheses and refined with fixed isotropic thermal parameters, $U_{iso}(H) = 1.2 \times U_{iso}(parent)$. All remaining hydrogens were included in calculated positions and assigned isotropic thermal parameters, $U_{iso}(H) = 1.2 \times U_{iso}(parent)$ or $U_{iso}(H) = 1.5 \times U_{iso}(C)$ for methyl groups.

Compound **3b** crystallized with two independent formula units in the asymmetric fraction of the unit cell. Moreover, **3b** crystallizes in the chiral space group $P2_1$; the value of the Flack parameter −0.11(5) indicates that the correct axial system was chosen to describe the structure.[19] Compound **6** co-crystallized with one molecule of CH_2Cl_2 which was disordered over three distinct sites in a 50 : 25 : 25 percent ratio. The various C–Cl bond distances were restrained to 1.75(2) Å using the SHELX DFIX card and the carbon atoms were refined with equivalent anisotropic thermal parameters.

CCDC reference numbers 192675–192677.

See http://www.rsc.org/suppdata/dt/b2/b208584b/ for crystallographic data in CIF or other electronic format.

Acknowledgements

We thank the Robert A. Welch Foundation for support (Grant AA-1201).

References

1 (*a*) R. N. Grimes, in *Comprehensive Organometallic Chemistry*, ed. G. Wilkinson, E. W. Abel and F. G. A. Stone, Pergamon Press, Oxford, 1982, vol. 1, section 5.5; (*b*) R. N. Grimes, in *Comprehensive Organometallic Chemistry II*, ed. E. W. Abel, F. G. A. Stone and G. Wilkinson, Pergamon Press, Oxford, 1995, vol. 1 (ed. C. E. Housecroft) ch. 9; (*c*) R. N. Grimes, *Coord. Chem. Rev.*, 2000, **200–202**, 773.

2 (*a*) S. A. Batten, J. C. Jeffrey, P. L. Jones, D. F. Mullica, M. D. Rudd, E. L. Sappenfield, F. G. A. Stone and A. Wolf, *Inorg. Chem.*, 1997, **36**, 2570; (*b*) I. Blandford, J. C. Jeffrey, P. A. Jelliss and F. G. A. Stone, *Organometallics*, 1998, **17**, 1402; (*c*) J. C. Jeffrey, P. A. Jelliss, L. H. Rees and F. G. A. Stone, *Organometallics*, 1998, **17**, 2258; (*d*) D. D. Ellis, A. Franken, P. A. Jelliss, F. G. A. Stone and P.-Y. Yu, *Organometallics*, 2000, **19**, 1993; (*e*) D. D. Ellis, A. Franken, T. D. McGrath and F. G. A. Stone, *J. Organomet. Chem.*, 2000, **614–615**, 208; (*f*) A. Franken, S. Du, P. A. Jelliss, J. A. Kautz and F. G. A. Stone, *Organometallics*, 2001, **20**, 1597; (*g*) S. Du, A. Franken, P. A. Jelliss, J. A. Kautz, F. G. A. Stone and P.-Y. Yu, *J. Chem. Soc., Dalton Trans.*, 2001, 1846.

3 V. N. Lebedev, D. F. Mullica, E. L. Sappenfield and F. G. A. Stone, *Organometallics*, 1996, **15**, 1669; J. C. Jeffery, V. N. Lebedev and F. G. A. Stone, *Inorg. Chem.*, 1996, **35**, 2967; J. C. Jeffrey, P. A. Jelliss, V. N. Lebedev and F. G. A. Stone, *Organometallics*, 1996, **15**, 4737.

4 S. Du, J. A. Kautz, T. D. McGrath and F. G. A. Stone, *Inorg. Chem.*, 2001, **40**, 6563.

5 S. Du, J. A. Kautz, T. D. McGrath and F. G. A. Stone, *J. Chem. Soc., Dalton Trans.*, 2002, 1553.

6 S. Du, J. A. Kautz, T. D. McGrath and F. G. A. Stone, *Inorg. Chem.*, 2002, **41**, 3202.

7 S. Du, J. A. Kautz, T. D. McGrath and F. G. A. Stone, *J. Chem. Soc., Dalton Trans.*, 2001, 2791.

8 L. I. Zakharkin and V. N. Kalinin, *Tetrahedron Lett.*, 1965, **7**, 407; M. F. Hawthorne, P. A. Wegner and R. C. Stafford, *Inorg. Chem.*, 1965, **4**, 1675; M. A. Fox, A. E. Goeta, A. K. Hughes and A. L. Johnson, *J. Chem. Soc., Dalton Trans.*, 2002, 2132.

9 D. D. Ellis, A. Franken, P. A. Jelliss, J. A. Kautz, F. G. A. Stone and P.-Y. Yu, *J. Chem. Soc., Dalton Trans.*, 2000, 2509.

10 E. L. Muetterties and C. W. Aleggranti, *J. Am. Chem. Soc.*, 1972, **94**, 6386.

11 D. D. Ellis, P. A. Jelliss and F. G. A. Stone, *Organometallics*, 1999, **18**, 4982; D. D. Ellis, J. C. Jeffery, P. A. Jelliss, J. A. Kautz and F. G. A. Stone, *Inorg. Chem.*, 2001, **40**, 2041.

12 F. H. Jardine, J. Rule and G. A. Vohra, *J. Chem. Soc. A*, 1970, 238.

13 W. H. Knoth, J. L. Little, J. R. Lawrence, F. R. Scholer and L. J. Todd, *Inorg. Synth.*, 1968, **11**, 33.

14 J. Plesek, T. Jelínek, E. Drdáková, S. Hermánek and B. Stíbr, *Collect. Czech. Chem. Commun.*, 1984, **49**, 1559.

15 J. C. Jeffery, P. A. Jelliss, J. Karban, V. N. Lebedev and F. G. A. Stone, *J. Chem. Soc., Dalton Trans.*, 1997, 1219.

16 R. B. King and F. G. A. Stone, *Inorg. Synth.*, 1963, **7**, 99.

17 SHELXTL version 5.03, Bruker AXS, Madison, WI, 1995.

18 G. M. Sheldrick, SHELXL-97, University of Göttingen, Germany, 1997.

19 H. D. Flack and G. Bernardinelli, *J. Appl. Crystallogr.*, 2000, **33**, 1143.